THE JOURNAL OF BIOLOGICAL CHEMISTRY VOL. 283, NO. 25, pp. 17083–17091, June 20, 2008

Peptide Specificity and Lipid Activation of the Lysosomal Transport Complex ABCB9 (TAPL)*

Received for publication, March 6, 2008, and in revised form, April 11, 2008 Published, JBC Papers in Press, April 22, 2008, DOI 10.1074/jbc.M801794200

Chenguang Zhao[‡], **Winfried Haase**[§], **Robert Tampé**[‡], **and Rupert Abele**[‡1]

From the [‡]*Institute of Biochemistry, Biocenter, Goethe-University Frankfurt, Max-von-Laue-Strasse 9, D-60438 Frankfurt am Main, Germany and* [§]*Structural Biology, Max-Planck-Institut for Biophysics, Max-von-Laue-Strasse 3, D-60438 Frankfurt am Main, Germany*

The lysosomal ABC transporter associated with antigen processing-like (TAPL, ABCB9) acts as an ATP-dependent polypeptide transporter with broad length selectivity. To characterize in detail its substrate specificity, a procedure for functional reconstitution of human TAPL was developed. By intensive screening of detergents, ideal solubilization conditions were evolved with respect to efficiency, long term stability, and functionality of TAPL. TAPL was isolated in a two-step procedure with high purity and, subsequently, reconstituted into proteoliposomes. The peptide transport activity of reconstituted TAPL strongly depends on the lipid composition. With the help of combinatorial peptide libraries, the key positions of the peptides were localized to the N- and C-terminal residues with respect to peptide transport. At both ends, TAPL favors positively charged, aromatic, or hydrophobic residues and disfavors negatively charged residues as well as asparagine and methionine. Besides specific interactions of both terminal residues, electrostatic interactions are important, since peptides with positive net charge are more efficiently transported than negatively charged ones.

ATP binding cassette (ABC)[2] transporters are one of the largest families of membrane proteins, found in all phyla of life. ABC transporters are involved in essential cellular processes, translocating a broad spectrum of substrates across membranes driven by ATP binding and hydrolysis (1). Their function or dysfunction has severe clinical impact, such as multidrug resistance in chemotherapy and cystic fibrosis (2). ABC transporters are composed of two transmembrane domains (TMDs) and two nucleotide-binding domains (NBDs) (3). The TMDs comprise the translocation pathway and, in the case of exporters, also the allocrite binding site. The NBDs bind and hydrolyze ATP, which drives allocrite transport across the membrane. In humans, 48 genes code for ABC proteins, which are divided into seven subfamilies (*ABCA* to *ABCG*) based on the homology of their NBDs (4).

ABCB9, also named TAPL (transporter associated with antigen processing-like), translocates peptides from the cytosol into the lumen of lysosomes driven by ATP hydrolysis (5). TAPL seems to be an ancient ABC transporter, since orthologs are found not only in vertebrates but also in invertebrates like *Caenorhabditis elegans* and in plants (6–8). TAPL is highly expressed in testis, moderately in brain and spinal cord, and at low levels in other tissues (9). On the cellular level, TAPL can be detected in HeLa cells and Sertoli cells as well as dendritic cells and macrophages, which are professional antigen-presenting cells (9–11). TAPL expression is strongly up-regulated during maturation of monocytes to dendritic cells as well as macrophages, implying its involvement in antigen presentation. However, TAPL is not part of the classical MHC class I-dependent pathway since it cannot restore MHC class I presentation in cells deficient in TAP (transporter associated with antigen presentation) (11).

TAPL is closely related to the endoplasmic reticulum-resident peptide transporter TAP, sharing 38 and 40% amino acid sequence identity with TAP1 and TAP2, respectively (9). Unlike the heterodimeric TAP complex, TAPL forms a homodimer. Each monomer is composed of an N-terminal TMD and a C-terminal NBD (5, 12). For peptide transport, ATP hydrolysis is essential, since nonhydrolyzable analogs cannot drive translocation (5). In contrast to TAP, TAPL functions as low affinity transporter, with a much broader length specificity than the TAP complex. The minimal size of peptides recognized by TAPL is a 6-mer. The longest substrate tested so far comprises 59 residues (5).

For detailed biochemical analysis of TAPL, we established for the first time the purification and functional reconstitution of this lysosomal peptide transport complex. Besides the optimization of solubilization, purification, and reconstitution, the phospholipid composition of proteoliposomes was adjusted for highest transport activity. Having this optimized system in hand allowed us to decipher the peptide specificity of TAPL on the single residue level. Using combinatorial peptide libraries, we determined the key peptide residues involved in TAPL recognition and, in a detailed screen, analyzed the amino acid preferences at these positions.

* This work was supported by the International Max-Planck-Research School for Structure and Function of Biological Membranes (to C. Z. and R. T.) The costs of publication of this article were defrayed in part by the payment of page charges. This article must therefore be hereby marked "*advertisement*" in accordance with 18 U.S.C. Section 1734 solely to indicate this fact.

[1] To whom correspondence should be addressed. Tel.: 49-69-798-29437; Fax: 49-69-798-29495; E-mail: abele@em.uni-frankfurt.de.

[2] The abbreviations used are: ABC, ATP-binding cassette; CHAPS, 3-[(3-cholamidopropyl)-dimethylammonio]-1-propanesulfonate; DDM, *n*-dodecyl-β-D-maltoside; DM, *n*-decyl-β-D-maltoside; DOPA, 1,2-dioleoyl-*sn*-glycero-3-phosphate; DOPC, 1,2-dioleoyl-*sn*-glycero-3-phosphocholine; DOPS, 1,2-dioleoyl-*sn*-glycero-3-phosphoserine; FOS-14, Fos-choline-14; MHC, major histocompatibility complex; NBD, nucleotide-binding domain; OG, *n*-octyl-β-D-glucopyranoside; PG, phosphatidylglycerol; PBR1 and -2, peptide-binding region 1 and 2, respectively; TMD, transmembrane domain; DOPE, 1,2-dioleoyl-*sn*-glycero-3-phosphoethanolamine.

EXPERIMENTAL PROCEDURES

Materials—Detergents, except for digitonin (Calbiochem), were purchased from Anatrace (Maumee, OH). The lipids were supplied by Avanti Polar Lipids (Alabaster, AL). Peptides and peptide libraries were synthesized by Fmoc (*N*-(9-fluorenyl)-methoxycarbonyl) solid phase chemistry (13). The polyclonal antibody to TAPL was raised against the C terminus of TAPL (^{750}DFTAGHNEPVANGSHKA^{766}) and epitope-purified from rabbit antiserum (5).

Membrane Preparation and Solubilization Screen—TAPL containing a C-terminal His_{10} tag or a Strep-tag II was expressed in Sf9 (*Spodoptera frugiperda*) insect cells infected with recombinant baculovirus (5). Sf9 cells were harvested by centrifugation (1,000 × *g*, 10 min, 4 °C) 48 h after infection. The cell pellets were washed with phosphate-buffered saline (137 mM NaCl, 2.7 mM KCl, 8.1 mM Na_2HPO_4, 1.8 mM KH_2PO_4, pH 7.4), snap-frozen in liquid nitrogen, and stored at −80 °C. For crude membrane preparation, cell pellets were thawed on ice in a volume of Tris buffer (10 mM Tris/HCl supplemented with 1 mM phenylmethylsulfonyl fluoride and 2.5 mM benzamidine, pH 7.4), equivalent to 10 times the volume of the cell pellet. Cells were disrupted by Dounce homogenization. To remove cell debris and nuclei, the samples were centrifuged at 1,000 × *g* for 10 min at 4 °C. Subsequently, crude membranes were pelleted by centrifugation of the supernatant at 20,000 × *g* for 30 min at 4 °C. The crude membranes were resuspended in HEPES buffer (20 mM HEPES, 140 mM NaCl, pH 7.5), and aliquots were snap-frozen in liquid nitrogen and stored at −80 °C. Protein concentration was determined by the Micro-BCA™ Protein Assay (Pierce).

To find the optimal detergent for solubilization, crude membranes were pelleted and resuspended in solubilization buffer (20 mM HEPES, 140 mM NaCl, 15% (w/w) glycerol, pH 7.5) supplemented with 1 mM phenylmethylsulfonyl fluoride, 2.5 mM benzamidine at a protein concentration of 5 mg/ml. Detergents were added to reach a ρ value of 2, where ρ is given as follows (14),

$$\rho = \frac{[\text{detergent}] - CMC}{[\text{lipid}]} \qquad \text{(Eq. 1)}$$

where *CMC* represents the critical micelle concentration of detergent. The lipid-to-protein ratio (w/w) was assumed to be 1, and the average molecular mass of a phospholipid was taken as 700 Da. After incubation with detergent for 30 min on ice, solubilized samples were centrifuged for 30 min at 100,000 × *g* at 4 °C. To determine the solubilization efficiency, the supernatants were analyzed by SDS-PAGE (10%) followed by immunoblotting using an epitope-purified anti-TAPL polyclonal antibody and quantified by chemiluminescence using a Lumi-Imager F1 from Roche Applied Science. The signals were normalized to the solubilization efficiency of crude membranes observed with 1% SDS.

Purification of TAPL—Crude membranes containing TAPL (5 mg/ml) prepared from Sf9 insect cells were solubilized in solubilization buffer containing 20 mM imidazole, 1 mM phenylmethylsulfonyl fluoride, 2.5 mM benzamidine, and 1% digitonin. After a 30-min incubation on ice and centrifugation (30 min at 100,000 × *g* at 4 °C), the supernatant was applied to an SP Sepharose™ Fast Flow column (GE Healthcare) equilibrated with binding buffer (20 mM HEPES, 140 mM NaCl, 20 mM imidazole, 15% (w/w) glycerol, and 0.1% digitonin, pH 7.5). The flow-through was loaded onto a Zn^{2+}-iminodiacetate column (Sepharose™) (GE Healthcare) equilibrated with binding buffer. After stringent washing with up to 100 mM imidazole, the specifically bound protein was finally eluted with elution buffer (20 mM HEPES, 140 mM NaCl, 250 mM imidazole, 15% (w/w) glycerol, and 0.1% digitonin, pH 7.5). The eluate was concentrated in a 100 kDa cut-off Amicon™ concentrator (Millipore, Schwalbach, Germany).

Reconstitution of TAPL—Lipids were dissolved in chloroform at 20 mg/ml and mixed in defined ratios (w/w). Chloroform was removed under reduced pressure on a rotary evaporator. The remaining lipid film was rehydrated in reconstitution buffer (20 mM HEPES, 140 mM NaCl, 5% (w/w) glycerol, pH 7.5) by bath sonification. To prepare homogenous large unilamellar vesicles, liposomes (10 mg/ml) were frozen in liquid N_2 and thawed at room temperature five times, followed by extruding 11 times through a 400-nm polycarbonate filter (Avestin, Mannheim, Germany) with an Avestin miniextruder. The liposomes were diluted to 2.5 mg/ml in reconstitution buffer and titrated with Triton X-100 until light scattering at 540 nm reached maximum. The Triton X-100-destabilized liposomes were mixed with the purified protein in a 40:1 ratio (w/w), unless specified otherwise, and incubated for 30 min at 25 °C under gentle agitation. For detergent removal, 40 mg/ml (wet weight) polystyrene beads (Bio-Beads SM-2; Bio-Rad) washed with methanol and water and equilibrated with reconstitution buffer were added successively four times. A Bio-spin column (Bio-Rad) was used to remove Bio-Beads, and proteoliposomes were pelleted by ultracentrifugation (300,000 × *g*, 45 min, 4 °C). Finally, the proteoliposomes (5 mg/ml lipids) were resuspended in reconstitution buffer.

Peptide Transport Assays—Peptide transport was performed either with fluorescein-labeled (15) or ^{125}I-labeled peptides (16). For peptide transport, proteoliposomes containing 1.25 μg of TAPL were preincubated with 5 mM $MgCl_2$ and 1 μM labeled peptide in 1× phosphate-buffered saline at 4 °C. Transport was initiated by adding 3 mM ATP and stopped by the addition of 200 μl of ice-cold stop buffer (1× phosphate-buffered saline, 10 mM EDTA) after incubation for 10 min at 37 °C if not mentioned otherwise. Subsequently, samples were transferred to microfilter plates preincubated with 0.3% polyethyleneimine (MultiScreen plates, Durapore membrane, 0.65-μm pore size; Millipore). Filters were washed twice with 250 μl of ice-cold stop buffer. The amount of radiolabeled peptide was quantified by a γ-counter (Beckman Coulter, Krefeld, Germany). If fluorescent peptides were used, the washed filters were incubated with 250 μl of elution buffer (1× phosphate-buffered saline, 1% SDS) for 5 min at room temperature. Fluorescent peptides were quantified by a fluorescence plate reader ($\lambda_{ex/em}$ 485/520 nm; Polarstar Galaxy, BMG, Offenburg, Germany). Background transport activity was measured in the absence of ATP.

Freeze Fracture Electron Microscopy—Proteoliposome preparations were placed between two small copper disks and rap-

idly frozen in liquid ethane. Replicas were prepared in a freeze fracture unit (BAF 400T; Balzers) and shadowed with platinum/carbon at an angle of 45°. Replicas reinforced by pure carbon were cleaned from organic material in chromosulfuric acid and analyzed by a Philips EM208S electron microscope.

RESULTS

Solubilization and Purification of TAPL—The complexity of biological membranes makes a detailed functional analysis of membrane proteins and intracellular transport processes extremely difficult. Therefore, purification and reconstitution of membrane proteins are required, a challenging task. It is of utmost importance to decipher the substrate specificity of the lysosomal transporter TAPL, since it is connected to its physiological function. Due to the high background and side reactions, it was impossible to resolve the substrate specificity in crude membranes. Therefore, a solubilization and reconstitution procedure was developed for this ABC transporter. Human TAPL with a C-terminal His_{10} tag was heterologously expressed with the baculovirus expression system. 48 h after infection of Sf9 insect cells with a multiplicity of infection of 2, cells were harvested, and crude membranes were prepared. Since solubilization by detergent is a critical step in membrane protein purification, we first screened for the optimal detergent for TAPL comparing the solubilization efficiency of the mild nonionic detergents digitonin, DDM, DM, OG, and Triton X-100 as well as the zwitterionic detergents FOS-14, CHAPS, and Zwittergent 3-12. TAPL was extracted from crude membranes with a detergent concentration equivalent to a ρ value of 2. After 30 min on ice, insoluble material was removed by ultracentrifugation. Solubilization efficiencies of different detergents were analyzed by SDS-PAGE and immunoblotting using a TAPL-specific antibody. The solubilization was normalized by the TAPL signal derived from SDS-treated crude membranes (Fig. 1). FOS-14 showed the highest solubilization efficiency (112%), followed by Zwittergent 3–12 (65%), Triton X-100 (65%), digitonin (56%), DDM (52%), CHAPS (40%), DM (34%), and finally OG (13%). Since detergent-solubilized membrane proteins can denature and aggregate over time, we tested the stability of TAPL after 3 days of storage at 4 °C in the detergent containing buffers. After removing aggregates by ultracentrifugation, soluble TAPL was analyzed by SDS-PAGE and immunoblotting (Fig. 1). TAPL stored for 60 h in digitonin, DDM, DM, Triton X-100, and FOS-14 did not precipitate, since the immunoblot signal stayed constant over time. However, in the presence of OG, CHAPS, and Zwittergent 3-12, roughly 50% of the solubilized TAPL precipitated and could not be detected in the soluble fraction over the same period. Previously, some detergents were reported to disrupt membrane protein complexes (17); therefore, the existence of TAPL homodimers in the presence of the stability-preserving detergents was analyzed by co-expression of TAPL with C-terminal His_{10} tag (TAPL-His) or with C-terminal Strep-tag II (TAPL-Strep) in Sf9 insect cells. TAPL was then solubilized using different detergents and isolated via the His tag of TAPL-His by Zn^{2+}-iminodiacetate-Sepharose. Importantly, TAPL-Strep could be co-precipitated with TAPL-His in the presence of Triton X-100, DDM, and digitonin, whereas DM and FOS-14 appeared to disrupt the TAPL complex (data not shown). For further studies, digitonin was used to extract TAPL from Sf9 crude membranes, because it had high solubilization efficiency, preserved the homodimeric complex, and, in particular, restored peptide transport activity after reconstitution (see below).

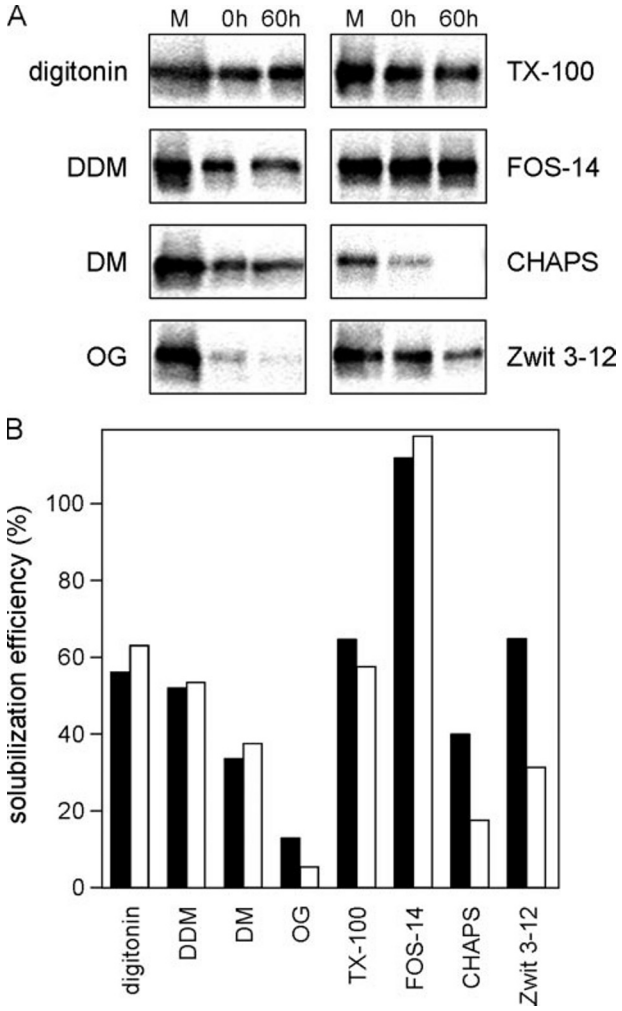

FIGURE 1. **Solubilization and stability of TAPL.** *A*, crude membranes (*M*) from insect cells (1.0 mg of total protein) were solubilized in 200 μl of solubilization buffer supplemented with detergents ($\rho = 2$) and proteinase inhibitors. After solubilization for 30 min on ice, the supernatant (0 h) was collected after ultracentrifugation (1 h; 100,000 $\times$ *g*), stored for 60 h at 4 °C, and centrifuged again, resulting in the second supernatant (60 h). Equal amounts of crude membrane solubilized in 1% SDS and both supernatants were analyzed by SDS-PAGE (10%) and subsequent immunoblotting using an epitope-purified anti-TAPL polyclonal antibody. *B*, immunoblot signals were quantified by chemiluminescence. The signals were normalized to the solubilization efficiency of crude membrane with 1% SDS. *Filled* and *open bars* symbolize TAPL in the supernatant after 0 and 60 h of solubilization. *TX-100*, Triton X-100.

Multistep protein purifications suffer from the drop of protein recovery with each step, and, in addition, the protein can be inactivated by surface interactions. Therefore, we established a gentle two-step method. First, impurities were removed by cation exchange chromatography without binding TAPL. Second, the flow-through from this step was loaded onto a Zn^{2+}-iminodiacetate matrix, where TAPL is specifically bound via its C-terminal His_{10} tag. After stringent washing with up to 100 mM imidazole, TAPL was eluted with 250 mM imidazole. By this

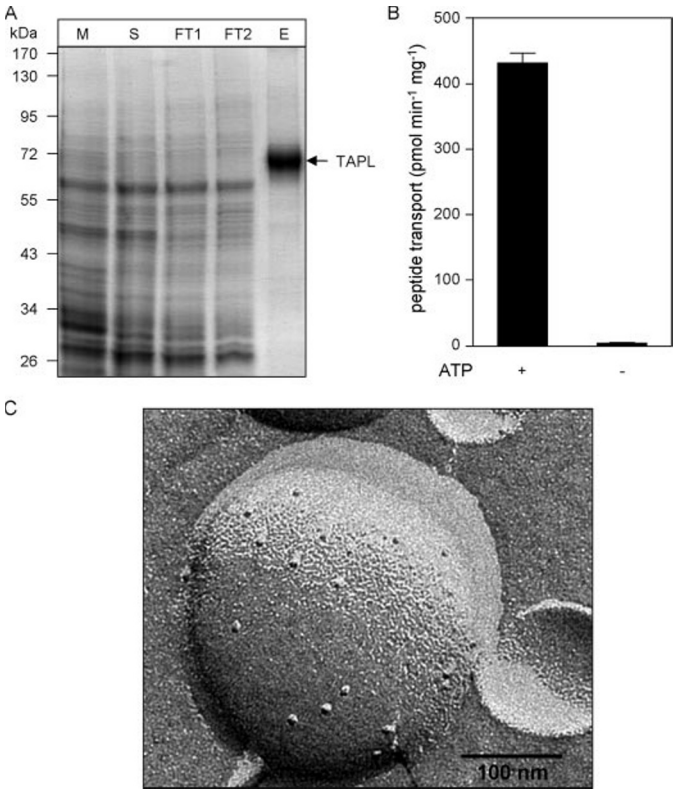

FIGURE 2. **Purification and reconstitution of TAPL.** *A*, purification of TAPL. Crude membranes (*M*) from insect cells (5 mg/ml) were solubilized in 1% digitonin. After centrifugation, the supernatant (*S*) was cleared from contaminations by cation exchange chromatography, whereas TAPL was left in the flow-through (FT1). In the second step, FT1 was applied to Zn^{2+}-iminodiacetate affinity chromatography. TAPL was not detected by SDS-PAGE (Coomassie-stained) in the flow-through (FT2) but rather in the eluate (*E*). *B*, ATP-dependent peptide transport of reconstituted TAPL. 50 μl of proteoliposomes (1.25 μg of TAPL in *E. coli* lipids) in PBS were incubated with 3 μM fluorescein-labeled peptide RRYCΦKSTEL (where Φ represents fluorescein coupled to cysteine) and 5 mM $MgCl_2$ in the presence or absence of 3 mM ATP for 10 min at 37 °C. After washing on filter plates, proteoliposomes were solubilized by SDS, and fluorescent peptides were quantified with a fluorescence plate reader ($\lambda_{ex/em}$ 485/520 nm). The experiments were performed in triplicate. *Error bars*, S.D. *C*, reconstitution of TAPL. After reconstitution via polystyrene beads, proteoliposomes were analyzed by freeze fracture electron microscopy. Particles indicate incorporation of protein into the membrane.

procedure, a yield of about 500 μg/liter cell culture of highly purified TAPL was obtained (Fig. 2*A*).

Functional Reconstitution of TAPL—Functional reconstitution of membrane proteins is a critical step depending on different parameters. Therefore, we optimized TAPL reconstitution into liposomes composed of *Escherichia coli* lipids for highest transport activity with respect to liposome preparation, destabilization of liposomes, lipid-to-protein ratio, and detergent removal. Substrate transport was determined with fluorescein-labeled peptide RRYCΦKSTEL (where Φ represents fluorescein coupled to cysteine) in the presence and absence of 3 mM ATP at 37 °C. The highest transport activity was obtained using large unilamellar liposomes, destabilized by Triton X-100 to the point of maximal light scattering, a lipid-to-protein ratio of 40:1 (w/w), and removal of detergents by serial addition of polystyrene beads (Fig. 2*B*). Membrane insertion was confirmed by freeze-fracture transmission electron microscopy, by which membrane incorporated particles are visible only after reconstitution of TAPL (Fig. 2*C*). After reconstitution into proteoliposomes, TAPL showed almost the same transport activity as in crude membranes, since the Michaelis-Menten constants for ATP ($K_{m,\mathrm{ATP}} = 98 \pm 28$ μM) and the fluorescein-labeled nonapeptide RRYCΦKSTEL ($K_{m,\mathrm{pep}} = 11 \pm 2$ μM) were in good agreement with those determined from crude membranes (5).

Lipid Activation of TAPL—The lipid composition is a critical parameter for the activity of reconstituted membrane proteins. Therefore, we screened different lipid compositions. Since TAPL is expressed in mammalian cells, we first compared the transport activity of TAPL reconstituted in liposomes derived from lipid extracts of bovine heart, brain, and liver with *E. coli* lipids. Surprisingly, TAPL was only active in *E. coli* lipids and not in any of the bovine lipid extracts (Fig. 3*A*).

Since the *E. coli* lipid composition differs drastically from the phospholipid repertoire in mammalian cells, we checked whether phosphatidylcholine, the most abundant phospholipid in eukaryotic cells, was suitable for functional TAPL reconstitution (18, 19). By mixing *E. coli* lipids with increasing concentrations of synthetic DOPC a bell-shaped curve for transport activity was detected with a maximal 3-fold increase at 30% of DOPC compared with pure *E. coli* lipids. At DOPC concentrations higher than 50%, the transport activity of TAPL is strongly decreased, whereas proteoliposomes of pure DOPC were inactive in peptide transport (Fig. 3*B*).

For two-dimensional crystallization as well as functional studies on the single-molecule level, it will be beneficial to work with a defined lipid mixture of pure phospholipids. Therefore, we reconstituted TAPL in liposomes containing a mixture of DOPC and either egg PG, DOPA, DOPS, or DOPE at a fixed ratio of 9:1 (w/w). Peptide transport was detected in liposomes containing DOPS or DOPA with a preference for DOPS (Fig. 3*C*). Proteoliposomes containing DOPE or PG were inactive in peptide transport. Next, TAPL activity in proteoliposomes composed of different ratios of DOPS and DOPC was analyzed to find the optimal phospholipid mixture (Fig. 3*D*). TAPL activity showed a bell-shaped dependence on the DOPS concentration with maximal transport at a DOPS/DOPC ratio of 1:1. These results demonstrate that TAPL activity is dependent not only on the charge but also on the specific head group of the phospholipids.

Key Positions for Substrate Recognition—TAPL has a broad peptide length specificity, ranging from 6-mer peptides up to at least 59-mer peptides (5). Peptides are recognized via their backbone, the free N and C terminus, and side chain interactions. To investigate peptide specificity on the single-residue level, we first focused on deciphering the key positions of the transported peptides. Thus, single cysteine-containing derivatives of the antigenic peptide RRYQKSTEL were labeled with 5-iodoacetamidofluorescein, which due to its size is expected to interfere with peptide transport. The position-dependent effects of this bulky fluorophor on ATP-dependent peptide transport can be grouped in four classes (Fig. 4*A*): (i) peptides labeled on the N- or C-terminal residue are not transported; (ii) the fluorophor at positions 2 and 3 interferes with peptide transport, in comparison with (iii) positions 4–7, and (iv) fluorescein at position 8 shows no reduction of the transport rate compared with radioactive labeled peptide and does not interfere with peptide transport.

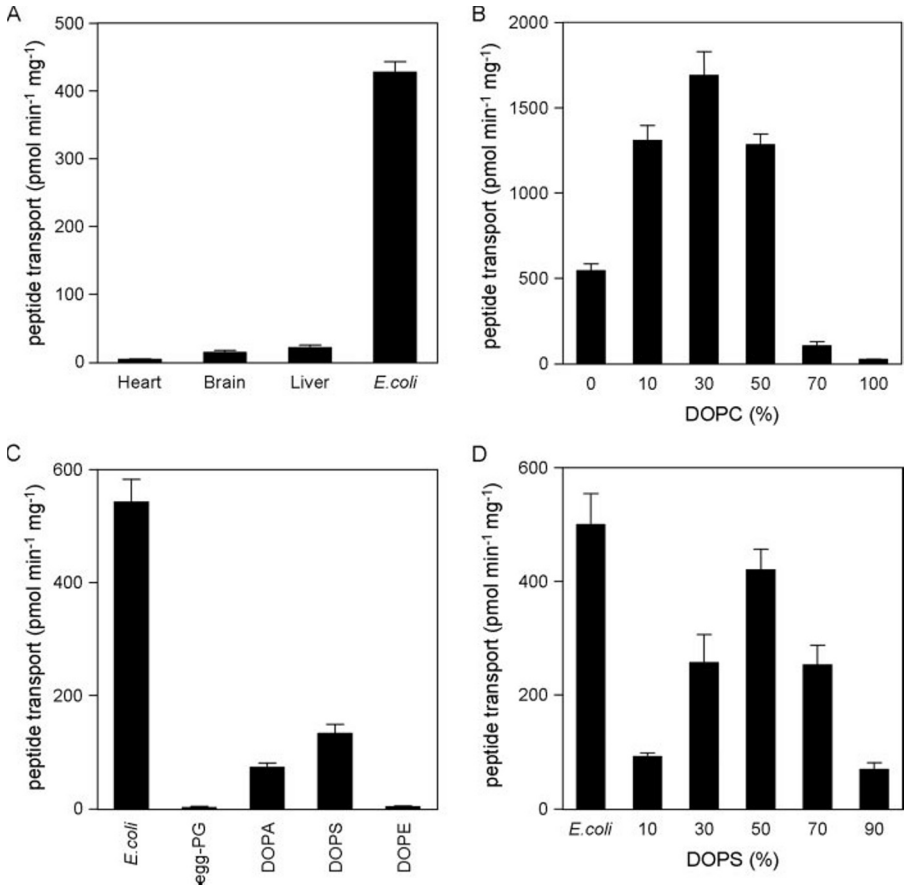

FIGURE 3. **Lipid activation of the lysosomal transport complex TAPL.** *A*, TAPL reconstituted in lipid extracts. Transport activity of TAPL reconstituted in liposomes prepared from bovine heart, brain, or liver lipids or *E. coli* lipids. *B*, phosphatidylcholine-dependent transport. TAPL was reconstituted in liposomes of *E. coli* lipids containing increasing concentrations of DOPC, and transport activity was quantified. *C*, reconstitution of TAPL in liposomes of defined lipid composition. Transport activity of TAPL reconstituted in liposomes composed of DOPC and either DOPA, DOPE, DOPS, or egg PG in a fixed ratio of 9:1 (w/w) was determined. For comparison, the activity of TAPL reconstituted in *E. coli* liposomes is given. *D*, phosphatidylserine-dependent transport. TAPL was reconstituted in liposomes composed of DOPC and increasing concentrations of DOPS, and transport activity was quantified. For comparison, activity of TAPL reconstituted in *E. coli* liposomes is given. Peptide transport was analyzed with fluorescein-labeled peptide as mentioned in the legend to Fig. 2. For ATP-dependent transport, the background signal obtained in the absence of ATP was subtracted from the fluorescence signal of peptide transport in the presence of ATP. The experiments were performed in triplicate. *Error bars*, S.D.

In order to further investigate residues critical for substrate recognition by TAPL, peptide transport was analyzed by using ^{125}I-labeled, totally randomized nonameric peptide libraries (X_9), which uncouples the studies from a specific peptide sequence context. In this combinatorial peptide library, all naturally occurring amino acids except cysteine are equally distributed at each position, as demonstrated by pool sequencing and mass spectrometry (20–22). First, peptide transport of peptide libraries with one D-amino acid at a given position was examined. These peptides differ only in the conformation of the side chain of this one residue in comparison with all of the L-peptide library, allowing us to detect the influence of a single position on transport. Peptide translocation was strongly impaired for peptide libraries with a D-amino acid at the N- or C-terminal position. However, randomized peptides with D-amino acids on all other positions except the N and C terminus showed transport rates comparable with the all L-peptide library (X_9). Notably, peptides with all D-amino acids are not transported by TAPL (5). Taken together, the data show that the N- and C-terminal residues are crucial for peptide recognition by TAPL, whereas the internal amino acids form only minor contacts with TAPL. Moreover, a bulky side chain at position 2 or 3 interferes with peptide transport most likely by steric hindrance.

Sequence Specificity of TAPL—To determine the amino acid preferences of the N- and C-terminal residues, we determined the transport rates of randomized peptide libraries with a defined amino acid at either the N or C terminus of the peptide (Fig. 5). Importantly, in this analysis, all observed transport rates were in the linear range and could be normalized to the transport of the totally randomized peptide library (X_9). In general, TAPL showed similar preferences for each of the termini. Positively charged, long hydrophobic residues and the aromatic side chains of Phe and Tyr at both positions are favored, whereas negatively charged residues as well as Asn and Met are disfavored. The differences in transport rates of favored and disfavored amino acid residues cover 2 orders of magnitude, and the differences are more pronounced for the C-terminal than the N-terminal position.

Since TAPL shows a broad length specificity ranging from 6-mer to at least 59-mer peptides, we tested whether this recognition pattern is length-independent. To do so, we determined peptide transport of a subset of randomized 6-mer peptide libraries with defined amino acids on the N- or C-terminal end resembling favored, disfavored, or intermediate amino acids (Fig. 6). Strikingly, the pattern of preference in transport rates normalized by X_6 library was very similar to the 9-mer libraries. Again, positively charged and aromatic residues at both ends are preferred, whereas negatively charged residues and Asn are disfavored. Moreover, as reflected by the higher variation, the C-terminal residue of the X_6 library has a stronger impact on transport than the N-terminal residue, also agreeing with the results from the X_9 library. However, the polar Ser residue at either end is disfavored in the X_6 library while favored in the X_9 libraries. In conclusion, the N- and C-terminal residues of the peptide constitute the key residues independent of the peptide size with a distinct preference for positively charged and aromatic amino acids.

To investigate the influence of a single amino acid on each residue of a nonameric peptide, we screened the transport efficiency of nonameric peptide libraries containing Arg or Asp at

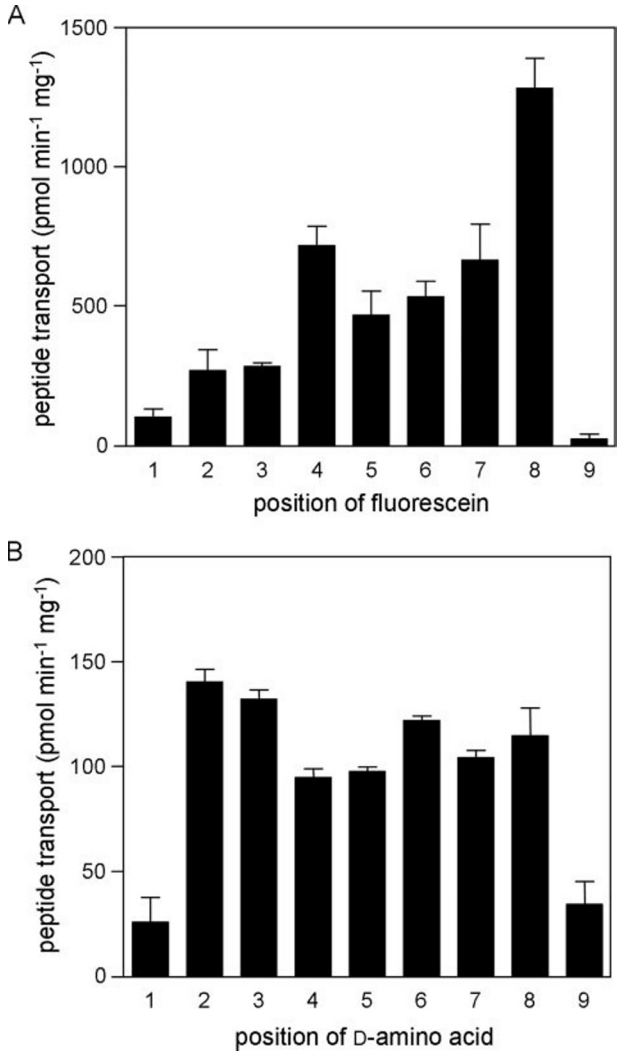

FIGURE 4. **Key position for peptide transport.** *A*, peptide transport of fluorescein-labeled peptides. Proteoliposomes containing TAPL (1.25 μg) were incubated in the presence or absence of 3 mM ATP with 3 μM derivatives of the nonapeptide RRYQKSTEL, in which each position was subsequently substituted with cysteine and labeled by iodoacetamidofluorescein. After 10 min at 37 °C, transport was stopped, and ATP-dependent peptide transport was quantified by fluorescence. *B*, peptide transport of combinatorial nonapeptide libraries. TAPL-dependent transport was determined in the presence of 1 μM radiolabeled, randomized peptide libraries containing one D-amino acid at a given position for 10 min at 37 °C. The ATP-dependent transport was quantified by γ-counting. The experiments were performed in triplicate, and the *error bars* show the S.D.

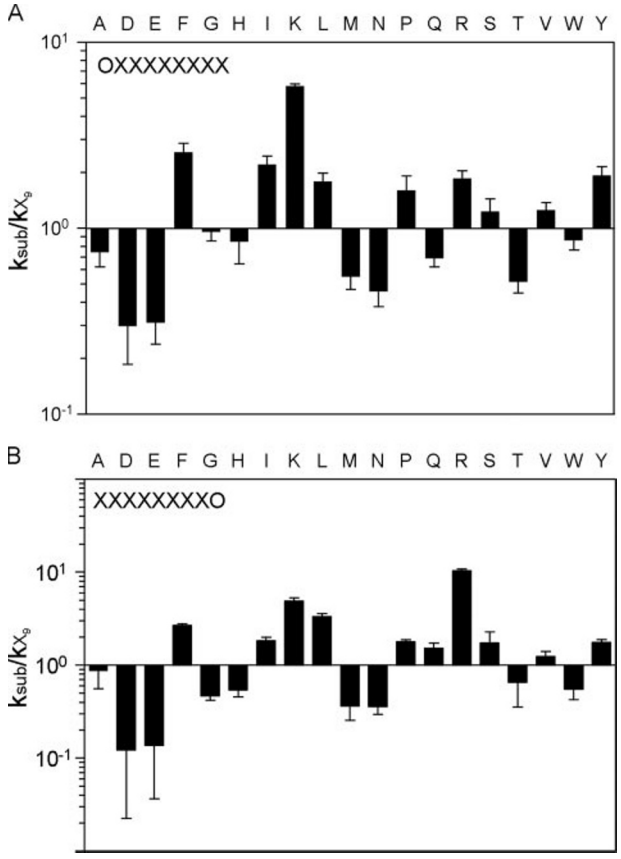

FIGURE 5. **Transport activity of N- and C-terminal randomized nonameric peptide sublibraries.** ^{125}I-Labeled, randomized nonapeptide sublibraries (1 μM) with defined N-terminal (*A*) or C-terminal (*B*) residues were incubated with proteoliposomes containing TAPL (1.25 μg) in the presence or absence of 3 mM ATP for 10 min at 37 °C. The ATP-dependent transport rates (k_{sub}) were normalized by the transport rate (k_{X_9}) obtained with the totally randomized peptide library X_9. The experiments were performed in triplicate, and the *error bars* show the S.D.

a defined position, since these residues showed the strongest influence on transport selectivity when present at either end (Fig. 7). All peptide libraries containing Arg showed a higher transport rate than the total randomized peptide library X_9 (Fig. 7*A*). Libraries with Arg at positions 1–8 were similarly efficient, whereas Arg at the C-terminal position doubled the transport rate in comparison with all other positions. The transport pattern of libraries containing Asp was very different from the Arg-containing libraries. Asp at positions 1–3 and especially position 9 disfavored transport (Fig. 7*B*). A negative charge at the remaining positions had only minor influence on peptide transport. The libraries containing Asp at position 4 or 8 exceeded slightly the transport rate of the X_9 library. The peptide transport of libraries containing Asp is reminiscent of the transport with the fluorescein-labeled peptides. In conclusion, TAPL prefers positively charged amino acids with the strongest effect on the C-terminal position, whereas negative charges at the three N-terminal positions or the C-terminal position are disfavored.

DISCUSSION

Based on systematic screens of various detergents for solubilization as well as optimization of purification and reconstitution procedures, we succeeded in the functional reconstitution of the human lysosomal transport complex TAPL, a milestone for the research on eukaryotic ABC transporters. In contrast to the multidrug transporters as well as lipid/cholesterol transporters reconstituted so far, TAPL transports hydrophilic peptides, which are easily quantified and are also good targets for systematic modifications. Therefore, this system represents an ideal starting point for mechanistic studies examining the stoichiometry between allocrite transport and ATP hydrolysis as well as the allocrite-transporter interaction by numerous biophysical approaches.

The functional reconstitution enabled us to decipher the substrate specificity of TAPL with the help of combinatorial peptide libraries. The key residues are restricted to the N- and

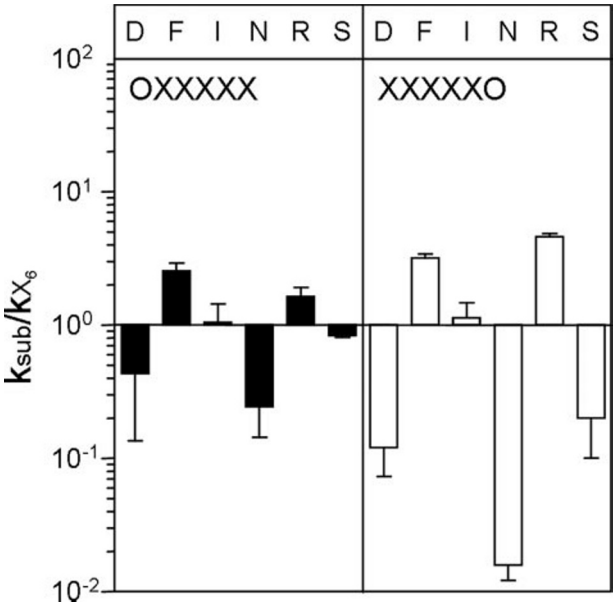

FIGURE 6. **Transport of randomized hexameric peptide sublibraries.** ^{125}I-Labeled, randomized hexameric peptide sublibraries (1 μM) with defined N-terminal or C-terminal residues were incubated with proteoliposomes containing TAPL (1.25 μg) in the presence or absence of 3 mM ATP for 10 min at 37 °C. The ATP-dependent transport rates (k_{sub}) were normalized by the transport rate (k_{X_6}) obtained with the totally randomized peptide library X_6. The experiments were performed in triplicate, and the *error bars* show the S.D.

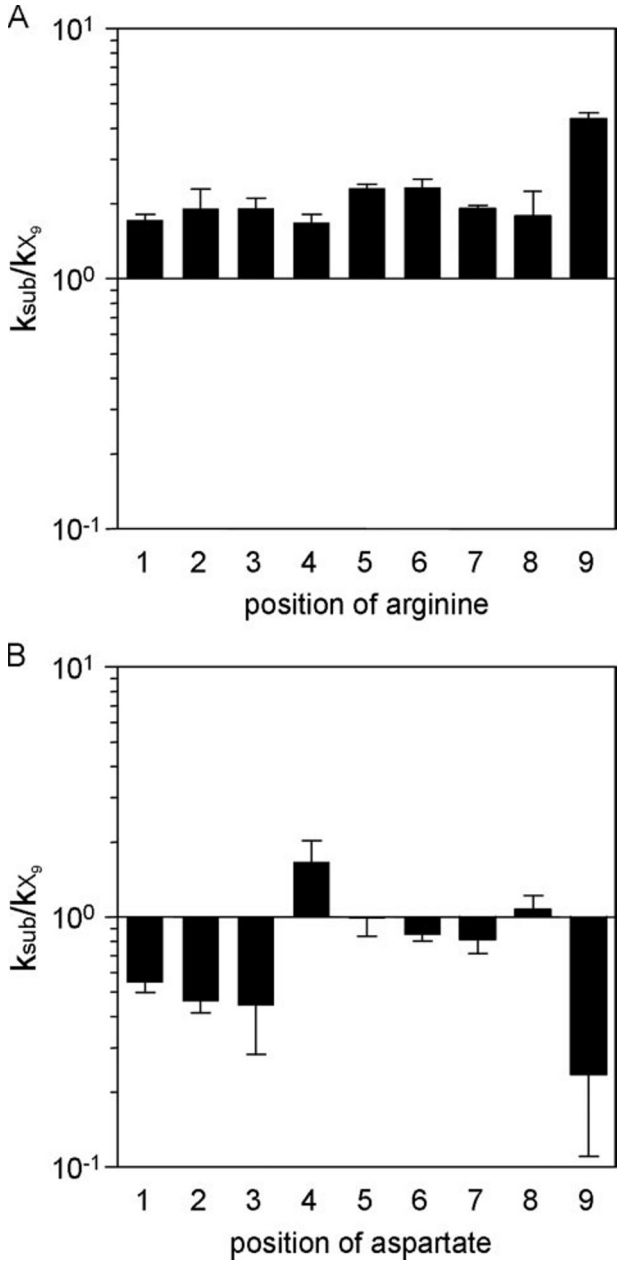

FIGURE 7. **Transport of nonameric sublibraries containing Arg or Asp at defined positions.** ^{125}I-Labeled, randomized peptide sublibraries (1 μM) containing Arg (*A*) or Asp (*B*) at a defined position were incubated with proteoliposomes containing TAPL (1.25 μg) in the presence or absence of 3 mM ATP for 10 min at 37 °C. The ATP-dependent transport rates (k_{sub}) were normalized by the transport rate (k_{X_9}) obtained with the totally randomized peptide library X_9. The experiments were performed in triplicate, and the *error bars* show the S.D.

C-terminal positions, of which positively charged, aromatic and large hydrophobic amino acids are preferred and negatively charged residues as well as Asn and Met are disfavored. Moreover, peptides with a positive net charge are favored in contrast to negatively charged peptides.

A prerequisite for the analysis of substrate specificity was the solubilization, purification, and reconstitution of TAPL. From the solubilization screen, digitonin, DDM, and Triton X-100 were the most powerful detergents with respect to efficiency, stability, and function of TAPL. OG, CHAPS, and Zwittergent 3-12 showed low solubilization efficiency paired with strong destabilization of TAPL. Short alkyl chain detergents and also zwitterionic detergents are beneficial for reconstitution because of their high critical micellar concentration. However, they often suffer from low solubilization efficiency as well as low long term stability of membrane proteins (23). FOS-14 and DM were acceptable as regards solubilization and stability but disrupted the homodimeric peptide transport complex. This also has been reported for other membrane proteins (17). A similar solubilization pattern was derived from TAPL expressed in Schneider cells (24).

To obtain the high purity of the transport complex required for biochemical and biophysical studies, a two-step purification procedure was applied. In the first step, impurities were removed by cation exchange chromatography. Since TAPL does not bind to the cation exchange matrix, denaturation of TAPL by surface contacts as well as its loss is minimized. In the second step, TAPL was isolated to more than 95% purity. The cation exchange step was essential to remove background ATPase activity[3] and is essential if precise quantification of the TAPL ATPase function is to be studied.

[3] C. Zhao, W. Haase, R. Tampé, and R. Abele, unpublished results.

The reconstitution was optimized with respect to yield and activity of TAPL. Given the mammalian origin of TAPL, it was surprising that TAPL was inactive when reconstituted in lipid extracts from bovine heart, brain, or liver but showed similar activity to crude membranes when reconstituted in *E. coli* lipid extracts. Whether the lack of transport activity in bovine lipid extracts is due to lipid composition, impurities in the extract, or incomplete sealing of the liposomes was not further investigated. The addition of DOPC to *E. coli* lipids substantially increased the transport activity of TAPL. Hence, phosphatidyl-

choline, which is the bulk phospholipid in most mammalian membranes, but absent in *E. coli* (18, 19), seems to have a stimulating effect on TAPL activity. Furthermore, introducing negatively charged phospholipids to pure DOPC increased TAPL activity. However, this is not only due to the negative charge of the lipid head group, since phosphatidylserine and phosphatidic acid are preferred, whereas no transport is detected with PG.

Based on the data presented herein together with our earlier study (5), the substrate specificity of TAPL has been deciphered. TAPL recognizes peptides via the N- and C-terminal residues and also the free N and C termini. The sequence in between can be highly variable in length and composition, allowing the translocation of a broad spectrum of peptides by one transporter. Clearly, the C-terminal position has the strongest effect on peptide selectivity, since modification at this position has the strongest impact on transport activity. Moreover, the variability at this position is also higher than at the N-terminal position. Positions 2 and 3 of the peptide seem to have minor effects on peptide selectivity. Those positions had no influence in the D-amino acid scan, whereas fluorescein or aspartate at these positions only marginally disfavored peptide transport. Since fluorescein as well as the side chain of Asp are negatively charged at physiological pH, electrostatic repulsion can cause decreased transport rates. Further electrostatic interactions appear to be responsible for the preferred transport of positively charged peptides. Two scenarios can be considered: (i) the environment of the peptide-binding pocket or the translocation pathway is negatively charged and therefore favors positively charged peptides, or (ii) the negatively charged membrane increases the local concentration of positively charged peptides in the vicinity of the transporter, which partially explains the dependence of peptide transport on the concentration of phosphatidylserine in the proteoliposomes.

Besides this global effect, there are also minor differences between the single positions. TAPL shows some preference for peptides with an Asp at position 4. Moreover, a peptide with a negatively charged fluorescein at position 4 is favored in transport. Therefore, it is feasible that the negative charge at this position is counterbalanced by positive charged residues in the peptide-binding pocket. Derived from the fluorescein scan, the second last position in the peptide seems to have a high degree of freedom. It could be conceivable that the side chain at this position does not stay in contact with TAPL but points into the liquid-filled environment.

The selectivity of TAPL and the related heterodimeric antigenic peptide transporter TAP, which share 40% sequence identity, show a strong overlap (9). Not only free N and C termini but also the key positions and selectivity principles are almost identical. Moreover, the C-terminal residue shows the highest impact on peptide selectivity (13, 25–29). However, there are distinct differences. Positions 2 and 3 of the peptide are also critical for recognition by TAP (13, 27, 30), whereas these residues have only a minor impact on TAPL selectivity. The importance of positions 2 and 3 for selectivity of TAP is slightly dependent on the method used for analysis. By peptide binding and competition assays, positions 2 and 3 show the same impact on TAP binding as position 1 (13, 27). However, by transport assays in semipermeabilized cells, which rely on trapping peptides in the endoplasmic reticulum by glycosylation, minor effects of positions 2 and 3 for peptide selectivity were detected (30).

TAPL transports peptides with a broad length specificity ranging from 6- to at least 59-mer but low affinity (5). In contrast, TAP translocates peptides between 8 and 16 amino acids in length with high affinity, whereas 6-mer peptides are no substrate (31–33). If the peptide selectivity of TAPL results from the binding step, as shown for TAP (15, 32, 34), the differences must reside in the binding pocket. Based on peptide photocross-linking studies and truncation studies, the peptide-binding region of TAP1 and TAP2 is localized at the cytosolic loop between transmembrane helix 4 and 5 of the core complex (peptide-binding region 1 (PBR1)) and a stretch of 15 residues C-terminal of the last transmembrane helix connecting the TMD with the NBD (PBR2) (35, 36). The substrate-binding pocket in the TAP complex seems to be formed between TAP1 and TAP2 subunits, since peptides neither bind to nor are transported by single subunits (33, 37), although homodimers can be formed (38).[4] Moreover, the asymmetry of the binding pocket restricts the orientation of the peptide, since TAP2 alleles in rats determine the selectivity for the C-terminal residue (25, 39, 40). In contrast, TAPL forms a homodimeric complex, which has no sequence-based asymmetry (5, 12). Interestingly, the putative PBR1 of TAPL shows a much higher sequence identity to TAP1 than TAP2, whereas PBR2 is more homologous to TAP2 than TAP1. Based on fluorescence cross-correlation spectroscopy experiments with TAP[5] and on the sequence comparison of both peptide transporters, we assume that TAP contains one peptide-binding site formed mainly by PBR1 of TAP1 and PBR2 of TAP2, whereas the two corresponding regions (PBR2 in TAP1 and PBR1 in TAP2) are inactive as regards binding. On the other hand, TAPL can bind one peptide simultaneously to each subunit, since two active peptide-binding pockets are present. The different modes of peptide binding could also explain the broader length specificity of TAPL in comparison with TAP.

TAPL expression is strongly up-regulated during the maturation of monocytes to dendritic cells or macrophages, where it is localized in the lysosomal compartment (11). There, it could be involved in the cross-presentation of antigenic peptides on MHC class I or II molecules. In the MHC class I cross-presentation pathway, exogenous antigens are taken up by pinocytosis or endocytosis by professional antigen-presenting cells and delivered to the cytosol (41–45). After proteasomal degradation, antigenic peptides could be transported via TAPL into lysosomes, where they are trimmed by proteases and subsequently bound to recycled MHC class I molecules for presentation on the cell surface. Similarly, cross-presentation of endogenous antigens by MHC class II is a process in which cytosolic proteins are degraded by the proteasome and the antigenic peptides are then transported by a TAP-independent pathway (perhaps via TAPL) into lysosomes for MHC class II loading (46, 47). It is likely, however, that TAPL has additional

[4] G. Oancea, R. Abele, and R. Tampé, unpublished data.
[5] M. Herget, R. Tampé, and R. Abele, unpublished data.

functions, since it is also expressed in the immunologically privileged tissues, such as brain and testis (9). Moreover, TAPL orthologs are also found in organisms that lack an adaptive immune system (6–8). There it could be involved in clearing proteins from the cytosol by chaperone-mediated autophagy (48), which is interestingly also found to participate in cross-presentation of antigenic peptides (49).

Acknowledgments—We thank Christine Le Gal as well as Drs. Joachim Koch and David Parcej for helpful discussions and for preparation of the manuscript. We thank Dr. Karl-Heinz Wiesmüller (EMC microcollections, Tübingen, Germany) for peptide libraries.

REFERENCES

1. Schmitt, L., and Tampé, R. (2002) *Curr. Opin. Struct. Biol.* **12,** 754–760
2. Borst, P., and Elferink, R. O. (2002) *Annu. Rev. Biochem.* **71,** 537–592
3. Biemans-Oldehinkel, E., Doeven, M. K., and Poolman, B. (2006) *FEBS Lett.* **580,** 1023–1035
4. Dean, M., Rzhetsky, A., and Allikmets, R. (2001) *Genome Res.* **11,** 1156–1166
5. Wolters, J. C., Abele, R., and Tampé, R. (2005) *J. Biol. Chem.* **280,** 23631–23636
6. Zhao, C., Tampé, R., and Abele, R. (2006) *Naunyn Schmiedeberg's Arch. Pharmacol.* **372,** 444–450
7. Uinuk-ool, T. S., Mayer, W. E., Sato, A., Takezaki, N., Benyon, L., Cooper, M. D., and Klein, J. (2003) *Immunogenetics* **55,** 38–48
8. Rea, P. A. (2007) *Annu. Rev. Plant. Biol.* **58,** 347–375
9. Zhang, F., Zhang, W., Liu, L., Fisher, C. L., Hui, D., Childs, S., Dorovini-Zis, K., and Ling, V. (2000) *J. Biol. Chem.* **275,** 23287–23294
10. Kobayashi, A., Hori, S., Suita, N., and Maeda, M. (2003) *Biochem. Biophys. Res. Commun.* **309,** 815–822
11. Demirel, Ö., Waibler, Z., Kalinke, U., Grünebach, F., Appel, S., Brossart, P., Hasilik, A., Tampé, R., and Abele, R. (2007) *J. Biol. Chem.* **282,** 37836–37843
12. Leveson-Gower, D. B., Michnick, S. W., and Ling, V. (2004) *Biochemistry* **43,** 14257–14264
13. Uebel, S., Kraas, W., Kienle, S., Wiesmuller, K. H., Jung, G., and Tampé, R. (1997) *Proc. Natl. Acad. Sci. U. S. A.* **94,** 8976–8981
14. Rivnay, B., and Metzger, H. (1982) *J. Biol. Chem.* **257,** 12800–12808
15. Neumann, L., and Tampé, R. (1999) *J. Mol. Biol.* **294,** 1203–1213
16. Chen, M., Abele, R., and Tampé, R. (2003) *J. Biol. Chem.* **278,** 29686–29692
17. Herget, M., Oancea, G., Schrodt, S., Karas, M., Tampé, R., and Abele, R. (2007) *J. Biol. Chem.* **282,** 3871–3880
18. DiRusso, C. C., and Nystrom, T. (1998) *Mol. Microbiol.* **27,** 1–8
19. van Meer, G., Voelker, D. R., and Feigenson, G. W. (2008) *Nat. Rev. Mol. Cell. Biol.* **9,** 112–124
20. Stevanovic, S., and Jung, G. (1993) *Anal. Biochem.* **212,** 212–220
21. Metzger, J. W., Kempter, C., Wiesmüller, K. H., and Jung, G. (1994) *Anal. Biochem.* **218,** 261–277
22. Wiesmüller, K.-H., Feiertag, S., Fleckenstein, B., Kienle, S., Stoll, D., Hermann, M., and Jung, G. (1996) in *Combinatorial Peptide and Nonpeptide Libraries: A Handbook for the Search of Lead Structures* (Jung, G., ed) pp. 203–246, Verlag Chemie, Weinheim, Germany
23. Seddon, A. M., Curnow, P., and Booth, P. J. (2004) *Biochim. Biophys. Acta* **1666,** 105–117
24. Ohara, T., Ohashi-Kobayashi, A., and Maeda, M. (2008) *Biol. Pharm. Bull.* **31,** 1–5
25. Heemels, M. T., Schumacher, T. N. M., Wonigeit, K., and Ploegh, H. L. (1993) *Science* **262,** 2059–2063
26. Momburg, F., Roelse, J., Howard, J. C., Butcher, G. W., Hämmerling, G. J., and Neefjes, J. J. (1994) *Nature* **367,** 648–651
27. van Endert, P. M., Riganelli, D., Greco, G., Fleischhauer, K., Sidney, J., Sette, A., and Bach, J. F. (1995) *J. Exp. Med.* **182,** 1883–1895
28. Grommé, M., van der Valk, R., Sliedregt, K., Vernie, L., Liskamp, R., Hämmerling, G. J., Koopmann, J.-O., Momburg, F., and Neefjes, J. J. (1997) *Eur. J. Immunol.* **27,** 898–904
29. Uebel, S., Meyer, T. H., Kraas, W., Kienle, S., Jung, G., Wiesmüller, K. H., and Tampé, R. (1995) *J. Biol. Chem.* **270,** 18512–18516
30. Neefjes, J., Gottfried, E., Roelse, J., Grommé, M., Obst, R., Hämmerling, G. J., and Momburg, F. (1995) *Eur. J. Immunol.* **25,** 1113–1136
31. Neefjes, J. J., Momburg, F., and Hämmerling, G. J. (1993) *Science* **261,** 769–771
32. Androlewicz, M. J., and Cresswell, P. (1994) *Immunity* **1,** 7–14
33. van Endert, P. M., Tampé, R., Meyer, T. H., Tisch, R. W., Bach, J. F., and McDevitt, H. O. (1994) *Immunity* **1,** 491–500
34. Gorbulev, S., Abele, R., and Tampé, R. (2001) *Proc. Natl. Acad. Sci. U. S. A.* **98,** 3732–3737
35. Nijenhuis, M., and Hämmerling, G. J. (1996) *J. Immunol.* **157,** 5467–5477
36. Ritz, U., Momburg, F., Pircher, H. P., Strand, D., Huber, C., and Seliger, B. (2001) *Int. Immunol.* **13,** 31–41
37. Meyer, T. H., van Endert, P. M., Uebel, S., Ehring, B., and Tampé, R. (1994) *FEBS Lett.* **351,** 443–447
38. Antoniou, A. N., Ford, S., Pilley, E. S., Blake, N., and Powis, S. J. (2002) *Immunology* **106,** 182–189
39. Wang, P., Gyllner, G., and Kvist, S. (1996) *J. Immunol.* **157,** 213–220
40. Powis, S. J., Young, L. L., Joly, E., Barker, P. J., Richardson, L., Brandt, R. P., Melief, C. J., Howard, J. C., and Butcher, G. W. (1996) *Immunity* **4,** 159–165
41. Houde, M., Bertholet, S., Gagnon, E., Brunet, S., Goyette, G., Laplante, A., Princiotta, M. F., Thibault, P., Sacks, D., and Desjardins, M. (2003) *Nature* **425,** 402–406
42. Guermonprez, P., Saveanu, L., Kleijmeer, M., Davoust, J., Van Endert, P., and Amigorena, S. (2003) *Nature* **425,** 397–402
43. Ackerman, A. L., Kyritsis, C., Tampe, R., and Cresswell, P. (2003) *Proc. Natl. Acad. Sci. U. S. A.* **100,** 12889–12894
44. Bachmann, M. F., Oxenius, A., Pircher, H., Hengartner, H., Ashtonrichardt, P. A., Tonegawa, S., and Zinkernagel, R. M. (1995) *Eur. J. Immunol.* **25,** 1739–1743
45. Monu, N., and Trombetta, E. S. (2007) *Curr. Opin. Immunol.* **19,** 66–72
46. Lich, J. D., Elliott, J. F., and Blum, J. S. (2000) *J. Exp. Med.* **191,** 1513–1524
47. Dani, A., Chaudhry, A., Mukherjee, P., Rajagopal, D., Bhatia, S., George, A., Bal, V., Rath, S., and Mayor, S. (2004) *J. Cell Sci.* **117,** 4219–4230
48. Majeski, A. E., and Dice, J. F. (2004) *Int. J. Biochem. Cell Biol.* **36,** 2435–2444
49. Zhou, D., Li, P., Lin, Y., Lott, J. M., Hislop, A. D., Canaday, D. H., Brutkiewicz, R. R., and Blum, J. S. (2005) *Immunity* **22,** 571–581